arXiv:1209.2607v1 [cond-mat.stat-mech] 12 Sep 2012

Universal properties of knotted polymer rings

M. Baiesi and E. Orlandini
Dipartimento di Fisica e Astronomia, Università di Padova, Via Marzolo 8, I-35131 Padova, Italy and Sezione INFN, Università di Padova, Via Marzolo 8, I-35131 Padova, Italy

(Dated: September 13, 2012)

By performing Monte Carlo sampling of N-steps self-avoiding polygons embedded on different Bravais lattices we explore the robustness of universality in the entropic, metric and geometrical properties of knotted polymer rings. In particular, by simulating polygons with N up to 10^5 we furnish a sharp estimate of the asymptotic values of the knot probability ratios and show their independence on the lattice type. This universal feature was previously suggested although with different estimates of the asymptotic values. In addition we show that the scaling behavior of the mean squared radius of gyration of polygons depends on their knot type only through its correction to scaling. Finally, as a measure of the geometrical self-entanglement of the SAPs we consider the standard deviation of the writhe distribution and estimate its power-law behavior in the large N limit. The estimates of the power exponent do depend neither on the lattice nor on the knot type, strongly supporting an extension of the universality property to some features of the geometrical entanglement.

PACS numbers: 36.20.Ey,02.10.Kn

I. INTRODUCTION

Scaling hypothesis and the renormalization group theory led to the understanding of universality in critical phenomena, i.e. the fact that systems that look different at small scales may share, in proximity of critical points, common statistical properties. This concept greatly reduces the variety of possible critical behavior by grouping all systems into a small number of universality classes characterized by the same critical exponents and critical amplitude ratios. In this respect universality justifies the study of systems in a given universality class that are simple enough to be treated either numerically or analytically.

In statistics of polymer conformations this approach has been often followed by modeling polymers as self-avoiding walks (SAWs) on discrete lattices such as the simple cubic (SC), the face-centered-cubic (FCC) and the body-centered cubic lattice (BCC). For these models combinatorial arguments and Monte Carlo simulations can be efficiently applied to obtain rigorous and numerical results on the large scale (asymptotic) behavior of polymers in good solution [1]. Moreover SAWs can be mapped to a magnetic system at its critical point and studied by renormalization group techniques [2, 3]. This approach has led, for example, to the well established results that the number $Z(N)$ and the mean squared radius of gyration $\langle R_g^2(N)\rangle_p$ of N-steps self-avoiding polygons (SAPs, i.e. $(N-1)$-steps SAWs having the two extremities one lattice distance apart) behave for large N respectively as

$$Z(N) \simeq A\mu^N N^{\alpha-2}\left(1+\frac{a}{N^{\Delta}}+\cdots\right) \qquad (1)$$

and

$$\langle R_g^2(N)\rangle_p \simeq BN^{2\nu}\left(1+\frac{b}{N^{\Delta}}+\cdots\right), \qquad (2)$$

where the amplitudes A, a, B, b, and the connective constant μ are non universal quantities that depend on the underlying lattice [1], while α and ν are universal exponents related by the hyperscaling equation $\alpha = 2-\nu d$ with d the dimensionality of the space and ν the metric exponent. In $d=3$, advanced numerical simulations give $\nu \simeq 0.587597(7)$ [4], and hence $\alpha \simeq 0.237209(21)$, in good agreement with field theoretical results [5]. Also the correction to scaling exponent Δ is believed to be universal and its best estimate is $\Delta = 0.528(12)$ [4].

Notice that SAPs on regular lattices model polymer rings in good solution with *any* possible topology, i.e. with an arbitrary number of knots tied in. However, in most experiments and physical situations such as in melts and concentrated solutions, the overall topology of a system of ring polymers cannot be changed unless the excluded volume interaction is violated. This, for example, has relevant consequences on the temperature of the collapse transition of ring polymers, which is found experimentally to be different from that of their linear counterparts [6].

Because of the topological constraint for looped polymers, the above mentioned mapping to a magnetic system is not valid anymore and, consequently, no field theory argument can establish the validity of scaling laws similar to (1) and (2). On the basis of previous numerical investigations [7–10] it is however reasonable to assume

$$Z_k(N) \simeq A_k\mu_k^N N^{\alpha_k-2}\left(1+\frac{a_k}{N^{\Delta_k}}+\cdots\right) \qquad (3)$$

and

$$\langle R_g^2(N)\rangle_k \simeq B_k N^{2\nu_k}\left(1+\frac{b_k}{N^{\Delta_k}}+\cdots\right), \qquad (4)$$

where μ_k and α_k are respectively the connective constant and the entropic exponent of the subset of SAPs with a given knot type k. With this notation k refers

either to prime knots or to composite knots given by the connect sum of prime knots (roughly speaking, a knot is composite if it can be split in two knots located in different portions of the chain, which are separated by a plane) [11, 12]. The case $k = \emptyset$ denotes the special case of unknotted SAPs (SAPs with trivial topology).

The scaling relations (3) and (4) have been conjectured in analogy with (1) and (2) and their validity has been confirmed so far only by numerical simulations [7, 11] with the findings $\mu_k = \mu_\emptyset < \mu$, $\alpha_k = \alpha_\emptyset + m_k$, $\nu_k = \nu$ and $B_k = B_\emptyset$ where m_k denote the number of prime components in the knot decomposition [11, 12]. The *probability* of occurrence of a given knot k,

$$P_k(N) = \frac{Z_k(N)}{Z(N)}, \tag{5}$$

is thus dominated by the exponential decay $(\mu_\emptyset/\mu)^N$ at large Ns. In the following we will not deal with this aspect but we will focus instead on the scaling beaviour of the ratios $P_k(N)/P_\emptyset(N) = Z_k(N)/Z_\emptyset(N)$.

It is important to stress that the exponent $\alpha_k = \alpha_\emptyset + m_k$ is consistent with the recent finding that prime knots in SAPs are weakly localized, i.e they occupy on average a portion of the ring that scales as N^t, with $t \simeq 0.7$ [13]. Indeed, given that each prime knot is weakly localized, SAPs with knot type k should, in the large N limit, look like as unknotted rings with m_k decorated vertices. These decorations can sit in $\sim N$ positions along the N-step SAP. The partition function of such decorated chain thus includes a scaling law N^{m_k} multiplying the partition function of unknotted chains, whose power-law part scales $\sim N^\alpha$. Similarly, the average extension of each prime component should not contribute, in the large N limit, to the overall extension of the knotted SAP and one would expect that SAPs with a fixed knot type k would share, to leading order, the same metric properties of unknotted SAPs [7].

A more recent numerical calculation of SAPs on the cubic lattice has confirmed and improved the above conjectures by suggesting the validity of the following scaling laws [14]

$$Z_k(N) \simeq Z_\emptyset(N) \times \frac{N^{m_k}}{C_k}, \tag{6}$$

where C_k is a coefficient growing with the knot complexity and factorizable into the elementary contributions of each prime component. Roughly speaking C_k can be interpreted as the elementary entropic cost to tie a given knot k in a SAP and its dependence on k can be related to the minimal number of steps necessary to build a knot type k on the underlying lattice [14]. Note that, for any two prime knots k_1 and k_2, the inverse proportionality relation $A_{k_1}/A_{k_2} = C_{k_2}/C_{k_1}$ is satisfied.

One of the aims of this work is to explore more deeply the scaling relation (6) by extending the numerical investigations in [14] to SAPs embedded both on BCC and FCC lattices and to look at the dependence of C_k on these lattices. While the value of C_k should depend on the three-dimensional lattice considered we expect the ratios $Z_{k_1}(N)/Z_{k_2}(N)$ to be independent on lattice details. This feature has been already suggested in [15] on the basis of a stochastic enumeration of N-steps SAPs performed with the GAS algorithm [16], an extremely efficient method to sample SAPs of moderate lengths and with fixed knot type. Note that the conclusions given in [15] rely on an extrapolation to infinity of the data obtained for SAPs within the range $N \leq 500$, i.e. in a region of Ns where, especially for knotted configurations, strong corrections to scaling are expected [17].

In this work we extend the range of sampled N up to 100000 by means of efficient Monte Carlo samplings. We have been able to compute the amplitudes C_k for different knot types and to confirm, for a wide range of N, the universal character of the ratios $Z_{k_1}(N)$ / $Z_{k_2}(N)$ found in [15] although with different asymptotic values.

In addition, by computing the mean squared radius of gyration of each SAP, we confirm, within a wide range of N, the validity of the scaling law (4). Finally, as a measure of the geometrical entanglement of knotted SAPs we have considered their writhe. Rigorous arguments have shown that, for SAPs on the cubic lattice, the mean absolute writhe $\langle |Wr| \rangle$ increases at least as rapidly as $\sqrt{N}$ [18] and numerical estimates on the same system gives $\langle |Wr| \rangle \sim N^\eta$ with $\eta = 0.5035 \pm 0.0006$ [19]. It is then natural to check whether, for SAPs with fixed knot type k, the scaling law for the spread of the writhe and the exponent η are independent either on the knot type k or on the underlying lattice.

II. MODELS AND METHODS

We perform Monte Carlo sampling of SAPs on the SC, BCC and FCC lattices by using the two-point pivot moves, a fixed-N algorithm that has been proven to be ergodic in the class of all SAPs and shown to be efficient in sampling uncorrelated configurations [1, 20, 21]. This algorithm allows us to reach values of N up to 10^5 for the BCC and FCC lattice. For the SC lattice instead we use previous data [14] including also $N = 1.5 \times 10^5$ and $N = 2 \times 10^5$. For the longest chains the samples include $\approx 2 \times 10^4$ independent configurations. For $N = 10^4$ this number raises to $\times 10^6$. Typically $> 10^5$ data are present for each N.

Since the pivot algorithm samples SAPs with any topology, it requires a post processing procedure to characterize the knot type of each configuration. This is can be determined, for example, by computing a topological invariant such as the Jones or the HOMFLY polynomials [22]. In general the computational complexity of these invariants increases exponentially with the geometrical entanglement of the curve and, for very large N, this could be the most problematic part of the whole investigation. To overcome this problem we first smooth each configuration by reducing its length while keeping the

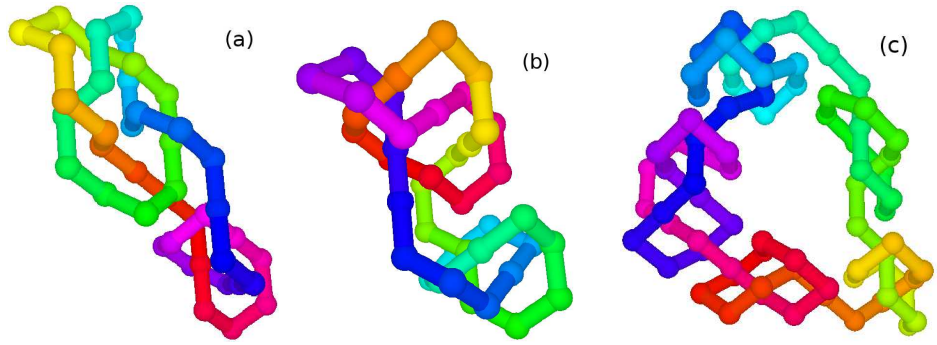

FIG. 1. (Color online) Examples of configurations obtained by the BFACF procedure that reduced their length from $N = 100000$ to a few steps, with the hue that follows the monomer sequence: (a) $3_1\#5_1$ knot on the BCC lattice, (b) $3_1\#5_1$ knot on the FCC lattice, and (c) a very tight configuration with knot type $(3_1)^4\#4_1$ on the BCC lattice.

knot type fixed. This is achieved by using a nonequilibrium stochastic scheme based on local moves (a nonequilibrium variant of the BFACF method [23–25]) that trims recursively all kinks in the SAP. In addition the algorithm performs some random local rearrangements to reduce the chance that a fast drop in chain length results into configurations which it is then very unlikely to escape from. This occurs for example when multiple prime components are present in the SAP and the resulting frozen configurations are characterized by having these components separated by stretched portions of the SAP that become difficult to shrink. We find that in most situations the algorithm is able to reach a configuration close to the minimal N allowed by its knot type on that specific lattice. This configuration is then projected along a given (approximately) irrational direction and the resulting knot diagram is mapped into the corresponding Dowker code [22] that is eventually further simplified and factorized into the Dowker codes of the prime knots. Finally, we compare each component of the original Dowker code against a look-up table of Dowker codes of prime knots of up to 11 crossings. In this way we have been able to distinguish composite knots with up to 5 prime components and with each prime component having minimal crossing number up to 11.

As an example of the efficiency of the simplification algorithm we show in Fig. 1 the result of the step reduction applied to configurations with $N = 100000$. The first two configurations display a $3_1\#5_1$ knot (i.e. a composite knot formed by a prime knot 3_1 and a prime knot 5_2), (a) on the BCC and (b) on the FCC lattice. One can readily see the $3_1\#5_1$ knot at these reduced lengths: the 3_1 part is on the lower-right side and the 5_1 part on the upper-left one. The configuration in Fig. 1(c) shows instead a $(3_1)^4\#4_1$ knot (this a shorthand notation for $3_1\#3_1\#3_1\#3_1\#4_1$). All these examples confirm the efficiency of the BFACF method in shrinking the chain from a very long length to a very short one, even for complex composite knots.

III. RESULTS

A. Frequencies of prime knots

The BCC and the FCC lattices have coordination number 8 and 12, respectively. It could be expected that more neighbors implies more flexibility and thus a more pronounced tendency to form knots. A manifestation of this effect would be that the knot costs C_k were somewhat inversely proportional to the coordination number. It turns out that indeed knots are less frequent in SAPs embedded on the SC lattice and hence $C_k^{\rm SC}$ is larger than its counterparts for FCC and BCC lattices. However, for the simplest knots we observe surprisingly that $C_k^{\rm BCC} < C_k^{\rm FCC}$. According to (6) this is readily seen by determining C_k from $NZ_\emptyset/Z_k$ for a simple prime knot. For instance, by focusing on C_{3_1} in [Fig. 2(a)] and C_{4_1} in [Fig. 2(b)] it is easy to see that these quantities are smaller for SAPs on the BCC lattice than on the FCC. If we consider instead the ratio Z_{3_1}/Z_{4_1} [Fig. 2(c)] we note that, as N increases,

	$C_k/10^5$			$C_k^{\rm SC}/C_k^{\rm L}$	
knot	SC	BCC	FCC	L=BCC	L=FCC
3_1	2.28(2)	1.57(1)	1.64(2)	1.45(2)	1.39(3)
4_1	50(1)	35.5(5)	37.5(5)	1.41(5)	1.33(5)
5_1	510(30)	378(18)	380(10)	1.35(14)	1.34(12)
5_2	334(15)	233(7)	257(10)	1.43(11)	1.30(11)
6_1	5700(1200)	3000(500)	3100(400)	1.9(7)	1.84(63)
6_2	6800(1900)	3450(600)	3500(400)	2.0(9)	1.94(77)
6_3	6900(1300)	5900(700)	6000(950)	1.17(36)	1.15(41)

TABLE I. Knot costs C_k for the SC, BCC, and FCC lattices, determined from averages of the data $NZ_\emptyset/Z_k$ in the range $5000 \le N < 100000$ (specific points clearly nonasymptotic for the knots with 6 crossings have also been excluded from the averages). Errors refer to one standard deviation. The ratios $Z_k^{\rm BCC}/Z_k^{\rm SC}$ and $Z_k^{\rm FCC}/Z_k^{\rm SC}$ in the last two columns seem to be independent on the knot k.

.

it approaches an asymptotic value that is independent on the lattice. This is true also for frequency ratios between other prime knots, as shown in Fig. 3 and in Table II. These results support the previously conjectures hypothesis that the frequency ratios between prime knots do not depend on the lattice in which they are embedded [15]. Our estimates in Table I and in Table II differ however from the ones reported in [15]. A possible explanation is that the estimates in [15] are affected by systematic errors due to the small values of N considered whose range fall in a region where the corrections to scaling are too strong (see the data for $N = 400$ in Fig. 2(c)) to be neglected.

Another way of presenting these results is by noticing that the frequencies of prime knots, whose inverse is proportional to the costs C_k, have fairly fixed ratios for different lattices: according to columns 5 and 6 of Table I, we see indeed that for each knot on the SC there are 1.44(3) knots on the BCC, and 1.37(3) knots on the FCC (these values correspond to weighted averages of the columns assuming a constant knot-independent ratio for the two lattices).

B. Frequencies of composite knots

The case of composite knots formed by $m_k = m$ topologically equivalent prime knots k (denoted $(k)^m$ hereafter), was recently discussed in [14] where the entropic cost $C_{(k)^m}$ was determined in a rather simple way in terms of the corresponding costs necessary to tie its prime components. Since each component is (weakly) localized, in the large N limit we can think of the chain with knot $(k)^m$ as an unknotted ring decorated by topologically identical objects (prime knots), each placed in one of $\sim N$ available locations. The entropic cost of each decoration is C_k, and being all independent one would expect that the full cost $C_{(k)^m}$ is simply given by the product of the m elementary costs C_k. However, in this picture, being the prime knots topologically identical, they can be interchanged along the chain keeping the configuration undistinguishable. This property gives rise to a combinatorial factor $m!$ that needs to be removed from the counting in order to define the relative entropy of the decorated chain with respect to the unknotted one. This gives

$$C_{(k)^m} = m!\,(C_k)^m. \tag{7}$$

For more general composite knots that include groups of different prime knots, the total cost is the product of the cost of each group given by (7).

For trefoil knots on the SC lattice is was shown that (7) was fulfilled by an excellent degree of precision [14]. In Fig. 4 we can see that also on FCC and BCC lattices the data follow the relation $Z_{(3_1)^m}/Z_\emptyset = N^m C_{(k)^m}$ with $C_{(k)^m}$ given by (7).

The importance of the factorial term $m!$ can be understood as follows: Since the trefoil is the prime knot with the lower cost C_k, one would first guess that SAPs with the composite knot $(3_1)^m$ are the most abundant ones for $N > C_{3_1}$. However, when the cost ratio C_{3_1}/C_{4_1} becomes

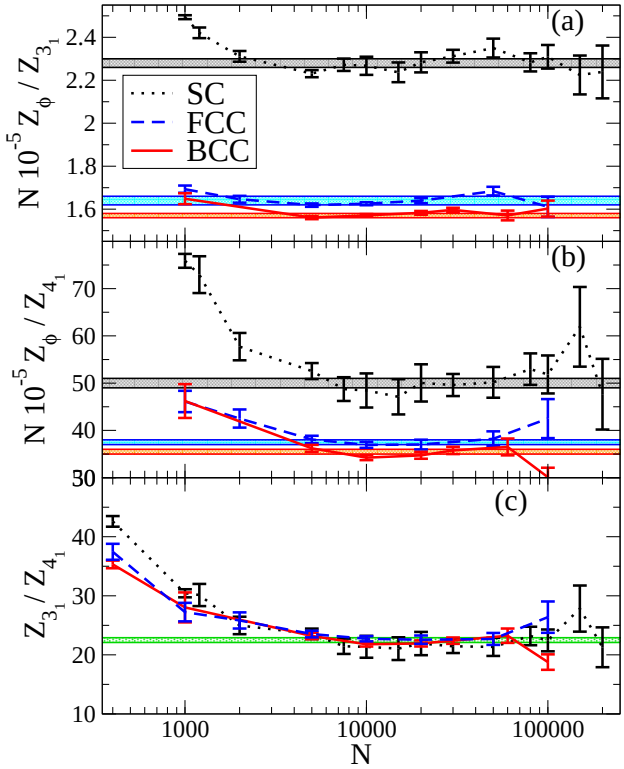

FIG. 2. (Color online) (a) Ratio of the probability of unknot configurations and of 3_1 knots, times $N \times 10^{-5}$. They converge to a lattice-dependent constant ($C_{3_1} \times 10^{-5}$) for large N. Bands of different colors represent the estimated asymptotic values with $\pm$ error, see Table I. (b) The same for knot 4_1. (c) Ratio of probability of 3_1 knot and of 4_1 knot, converging to a constant for large N (C_{4_1}/C_{3_1}) that does not depend on the lattice kind. The horizontal lines mark the interval of the estimated asymptotic value, see Table II. This panel includes also data at $N = 400$. Note that, while the small N deviations from the asymptotic values are due to corrections to scaling, the fluctuations at larger N's are originated by limited statistics.

		$Z_{k_1}/Z_{k_2} = C_{k_2}/C_{k_1}$			
k_1	k_2	SC	BCC	FCC	mean
3_1	4_1	21.9(7)	22.6(5)	22.9(6)	22.5(4)
3_1	5_1	224(15)	241(13)	231(9)	232(9)
3_1	5_2	146(8)	149(6)	157(8)	150(5)
3_1	6_1	2500(550)	1900(350)	1900(300)	2000(300)
3_1	6_2	3000(900)	2200(400)	2100(300)	2200(400)
3_1	6_3	3000(600)	3750(500)	3650(650)	3500(400)

TABLE II. Ratios of partition function of 3_1 and of other simple prime knots k_2 (i.e. C_{k_2}/C_{3_1}), for the three lattices, showing independence on the lattice type.

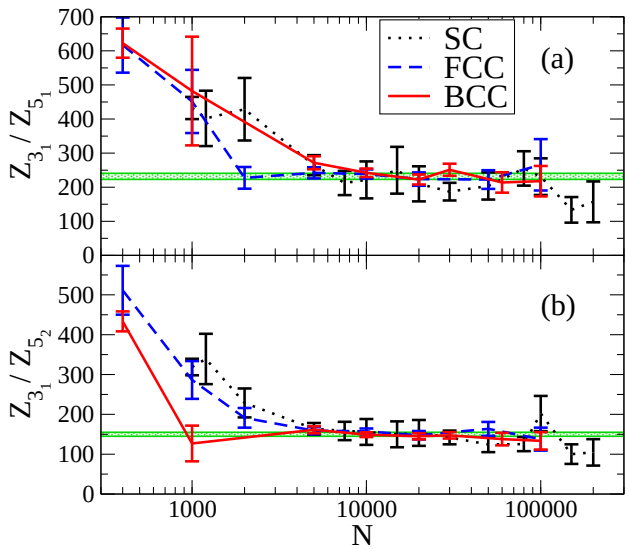

FIG. 3. (Color online) Ratio of probability of 3_1 knot and of (a) 5_1 knot, (b) 5_2 knot. The horizontal lines represent the estimated asymptotic ratio (Table II, last column) $\pm$ error.

smaller than m, because of the factorial factor $m!$, configurations with knot $(3_1)^{m-1}\#4_1$ are more frequent than those hosting the knot $(3_1)^m$. Since $C_{3_1}/C_{4_1} \approx 22$ this means that the combinatorial entropy loss should start to become relevant for a number of prime components $m \gtrsim 22$, which corresponds to $N \approx (C_{3_1})^{22}$, i.e. chain lengths (for example, $N \approx 10^{114}$ on the BCC lattice) that are impossible to test numerically. Hence, we can safely expect trefoils to dominate the knot statistics for realistic polymer rings in good solvent regime.

C. Metric properties

By collecting sampled configurations with the same knot type we can compute, for example, the mean squared radius of gyration $\langle R_g^2(N)\rangle_k$ of SAPs with fixed topology and see if its scaling behavior depends either on k or on the lattice in which the SAPs are embedded. According to (4) we consider the ratio $\langle R_g^2(N)\rangle_k/N^{2\nu} \sim B_k(1+b_k/N^{\Delta})$ and assume $\Delta = 1/2$ that is close to all present estimates [4]. In Fig. 5 we report these ratios as a function of $N^{-1/2}$ for $\nu = 0.587597$ [4] and for different knot types: one can readily see that these ratios converge (as $N \to \infty$) to a common value, independent on the knot type. This supports the expectation that B_k is the same for all knots [7] and confirms indirectly the weak localization property of the knotted portion of the chain [13]. The value of B_k does however depend on the chosen lattice and is larger on the BCC [≈ 0.28, see Fig. 5(a)] than on the FCC [≈ 0.18, see Fig. 5(b)]. This is somehow expected since B_k is an amplitude. Note that, while B_k does not depend on topology, this is not true

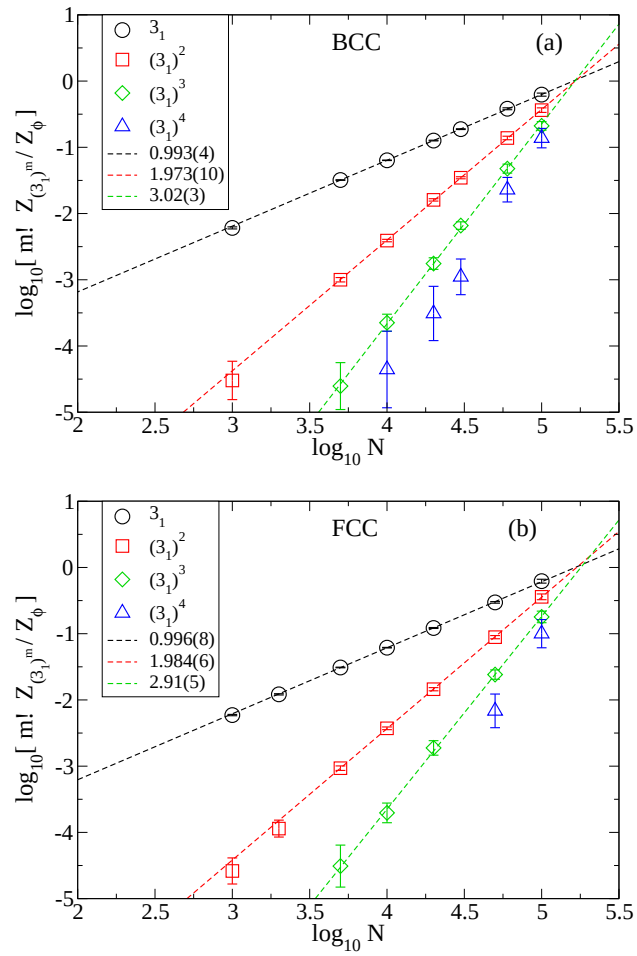

FIG. 4. (Color online) Log-log plot of ratios of partition functions $Z_{(3_1)^m}/Z_\emptyset$ vs. N, for multiple trefoil knots, in (a) the BCC lattice and (b) the FCC lattice. The straight lines are fits compatible with power laws N^m (exponents are in the legend). For each lattice, the crossing of these power-laws is at a single point of coordinates $(C_{3_1}, 1)$.

for the amplitude of the correction to scaling b_k whose value increases with knot complexity.

D. Writhe

The writhe of a curve is a quantity that describe its geometrical self-entanglement. A commonly used algorithm to compute the writhe of a curve goes as follows: First, one projects the curve onto an arbitrary plane. In general the projection will have crossings that most of the time will be transverse, so that, after having established an orientation of the curve, a sign $+1$ or -1 (determined by a right hand rule) can be assigned to each crossing. The sum of these signs gives the signed crossing number in this projection. The writhe of the curve is obtained by averaging these signed crossing numbers over all possible projections. From this definition it is

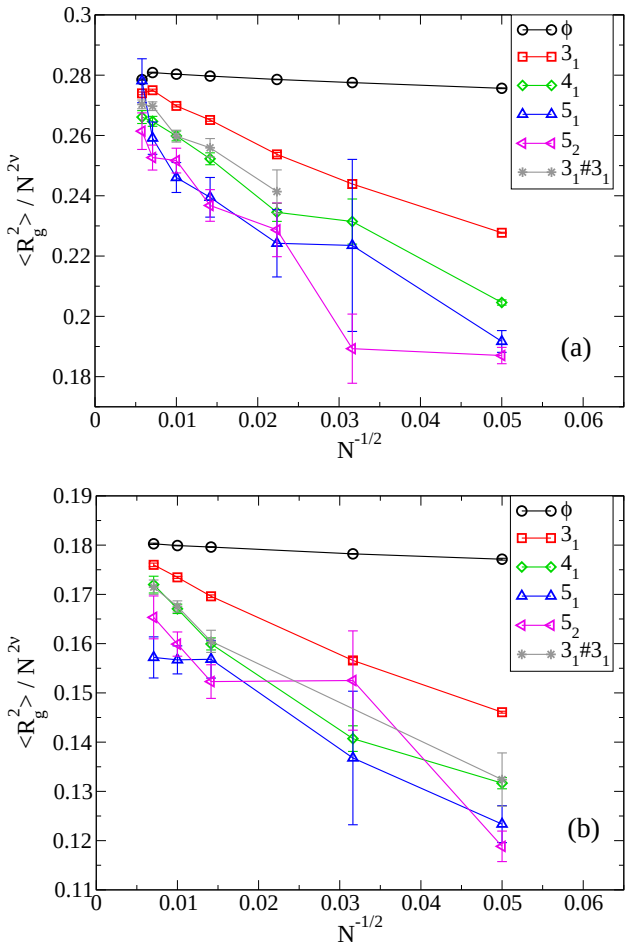

FIG. 5. (Color online) Mean radius of gyration $\langle R_g^2 \rangle$ divided by $N^{2\nu}$, with $\nu = 0.587597$, i.e. corrections to scaling of $\langle R_g^2 \rangle$ as a function of $N^{-1/2}$: (a) BCC lattice and (b) FCC lattice. Note that error bars and fluctuations for knots 5_1 and 5_2 at $N = 1000$ are larger than other ones because of worse statistics.

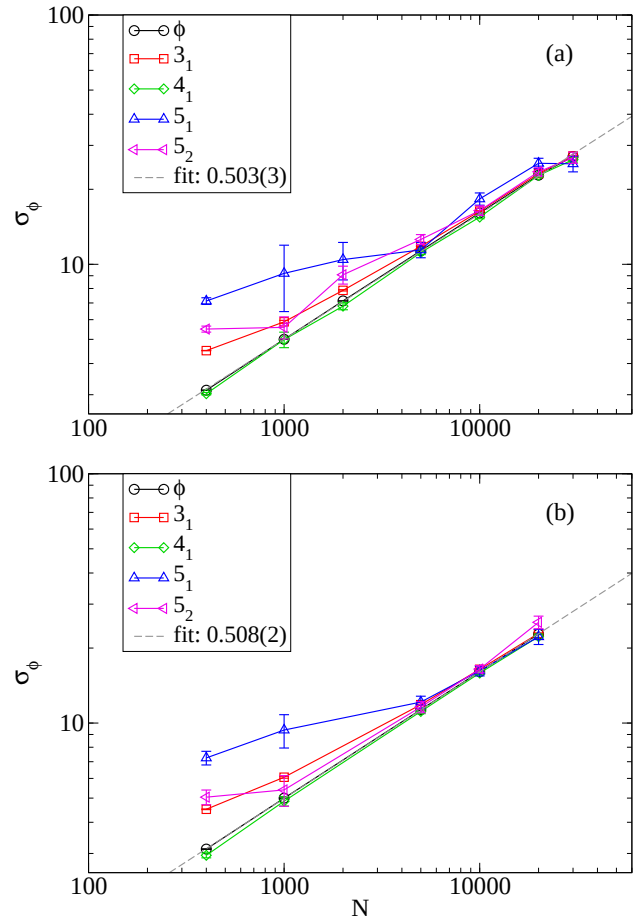

FIG. 6. (Color online) Log-log plot of the standard deviation of the writhe distribution as a function of N: (a) BCC lattice and (b) FCC lattice.

clear that the main difficulty in computing the writhe of a configuration would be the averaging procedure over all projections. Fortunately, for polygons on SC, FCC and BCC this procedure is enormously simplified by theorems [26–28] which reduce the computation of writhe to the average of linking numbers of the given curve with a finite set of selected push-offs of the curve itself. In our calculation of the writhe we made extensive use of these results.

Clearly the writhe of SAPs is, on average, zero and, provided we do not distinguish mirror images in chiral knots, this is still true for SAPs with fixed knot type. The simplest non trivial observable for the writhe distribution of SAPs with knot type k is then its standard deviation σ_k. In Fig. 6 we report the log-log plot of several σ_k as a function of N. Different symbols refer to different knot types and it is readily seen that, for sufficiently long N all data converge to a common curve that is essentially the one for unknotted SAPs. We can then argue that, similarly to SAPs in the SC lattice [19], and for all the knots considered here $\sigma_k \sim \sigma_\emptyset = D_\emptyset N^{\eta_\emptyset}$, both for FCC and BCC lattices.

A simple linear fit of the log-log data gives estimates $\eta_\emptyset = 0.503(3)$, $D_\emptyset = 0.155(5)$ for BCC and $\eta_\emptyset = 0.508(2)$, $D_\emptyset = 0.1495(14)$ for the FCC. These estimates are quite consistent with the estimate $\eta_\emptyset = 0.506(1)$ found for the SC lattice [19]. This is not true, however, for the amplitude $D_\emptyset$ whose estimate in the SC ($D_\emptyset = 0.1369(7)$) differs from the ones shown above for the other two lattices.

Similar results are found for the absolute value of the writhe (exponent $\eta_\emptyset = 0.504(4)$ on the BCC and $\eta_\emptyset = 0.508(2)$ on the FCC), which is expected, given the regular shape of the writhe distribution [19].

Two features are worth noticing: firstly the estimate of $\eta_\emptyset$ is very close to the lower bound 1/2 proved rigorously for SAPs with free topology in the SC lattice [18]. Secondly the deviation from the scaling law experienced

by SAPs with fixed knot type is less pronounced for the figure-eight and the unknot (achiral) then for all the others knots that are chiral. This is related to the nonzero mean writhe of each of the two images of a chiral knot, see [19].

IV. DISCUSSION

Since renormalization group arguments are not applicable to the statistical ensembles of rings with fixed knot type, we have resorted to simulations to investigate the universal features of the scaling laws for the entropic, metric and geometrical properties of knotted SAPs. We have confirmed that frequencies of knots in SAPs depend on the lattice in which the configurations are embedded, On the other hand the ratios between knot frequencies are lattice-independent numbers and depend only on the knot types involved. Surprisingly, knotted configurations are more frequent on the BCC than on the FCC lattice. This finding is unexpected because the FCC lattice has a higher coordination number than the BCC one, and because the knots with the shortest number of steps are found in the FCC lattice [15].

We have also supported the conjecture that composite knots in SAPs appear with frequencies that, in the large N limit, can be inferred from those of the prime knots in the knot decomposition. This property was conjectured for polygons on the cubic lattice [14] and here is confirmed also for SAPS on the BCC and FCC lattices. The composite *knot cost* includes a factorial $m!$ for every group of m identical prime knots, which multiplies the m-th power of their cost. The factorial term is suitable to properly take into account the combinatorial entropic loss for identical prime components in the picture where, in the large N limit, each prime component behaves as a decorating point along the unknotted ring. As a byproduct one can predict that, for chain lengths $N > 10^{114}$, knots with the highest frequency include not only trefoil knots but also other prime knots.

Concerning the metric properties of SAPs with fixed topology, our results for all the three lattices considered confirm that not only does the mean squared radius of gyration share the usual power law $N^{2\nu}$ known for the set of all SAPs but also the amplitude B_k does not depend on the knot type k [7], see (4). The dependence on the knot type is however present at the level of the corrections to scaling, which become more pronounced as the knot complexity of the SAPs increases.

Finally we have shown that the large N scaling behavior of the variance of the writhe (or equivalently its absolute value) for SAPs with knot type k is independent both on k and lattice type and is very close to $\sqrt{N}$, which is the lower bound proved by rigorous arguments for the class of all SAPs on the SC lattice [18].

By universality it is reasonable to expect that most of the features shown here for SAPs on lattices can be valid also for other models of polymer rings in which the excluded volume interaction is taken into account. On the other hand preliminary studies on the knot probability for off-lattice rings have either neglected completely the excluded volume interaction [29] or looked at the knot probability amplitudes for few and rather small values of N [30] . In the near future it would be then interesting to extend the analysis reported here to a larger set of polymer models.

[1] N. Madras and G. Slade, *The Self-Avoiding Walk* (Birkhäuser, 1993).
[2] P.-G. de Gennes, *Scaling concepts in Polymer Physics* (Cornell University Press, Ithaca, New York, 1979).
[3] C. Vanderzande, *Lattice Models of Polymers* (Cambridge University Press, 1998).
[4] N. Clisby, Phys. Rev. Lett. **104**, 055702 (2010).
[5] R. Guida, J. Zinn-Justin, J. Phys. A: Math. and Gen. **31**, 8103 (1997).
[6] A. Takano, Y. Kushida, Y. Ohta, K. Masuoka, and Y. Matsushita, Polymer **50**, 1300 (2009).
[7] E. Orlandini, M.C. Tesi, E. J. Janse van Rensburg, S. G. Whittington, J. Phys. A: Math. Gen. **31**, 5953 (1998).
[8] B. Marcone, E. Orlandini, A. L. Stella, F. Zonta, Phys. Rev. E **75**, 041105 (2007).
[9] E. Rawdon, A. Dobay, J. C. Kern, K. C. Millett, M. Piatek, P. Plunkett, and A. Stasiak, Macromol. **41**, 4444 (2008).
[10] E. J. Janse van Rensburg, A. Rechnitzer, J. Phys. A: Math. Theor. **41**, 105002 (2008).
[11] E. Orlandini, M. C. Tesi, E. J. Janse van Rensburg, S. G. Whittington, J. Phys. A: Math. Gen. **29**, L299 (1996).
[12] E. Orlandini, S. G. Whittington, Rev. Mod. Phys. **79**, 611 (2007).
[13] B. Marcone, E. Orlandini, A. L. Stella, F. Zonta, J. Phys. A: Math. Gen. **38**, L15 (2005).
[14] M. Baiesi, E. Orlandini, A. L. Stella, J. Stat. Mech. **10**, P06012 (2010).
[15] E. J. Janse van Rensburg, A. Rechnitzer, J. Phys. A: Math. Theor. **44**, 162002 (2011).
[16] E. J. Janse van Rensburg, A. Rechnitzer, J. Phys. A: Math. Theor. **42**, 335001 (2009).
[17] M. Baiesi, G. T. Barkema, and E. Carlon, Phys. Rev. E. **81** (2010).
[18] E. J. J. V. Rensburg, E. Orlandini, D. Sumners, M. C. Tesi, and S. G. Whittington, J. Phys. A: Math. Gen. **26**, L981 (1993).
[19] M. Baiesi, E. Orlandini, S. G. Whittington, J. Chem. Phys. **131**, 154902 (2009).
[20] N. Madras, A. Orlitsky, L. A. Shepp, J. Stat. Phys. **58**, 159 (1990).
[21] E. J. Janse van Rensburg, N. Madras, S. Whittington, J. Phys. A: Math. Theor. **23**, 1589 (1990).
[22] C. C. Adams, *The Knot Book* (Freeman, 1994).
[23] B. Berg, D. Foester, Phys. Lett. B **106**, 323 (1981).
[24] C. Aragao de Carvalho, S. Caracciolo, J. Fröhlich, Nucl.

Phys. B **215**, 209 (1983).
[25] E. J. Janse van Rensburg, S. G. Whittington, J. Phys. A: Math. Gen. **24**, 5553 (1991).
[26] R. Lacher, D. W. Sumners, Computer simulation of Polymers, ed R.J. Roe , 365 (1991).
[27] M. Garcia, E. Ilangko, S. G. Whittington, J. Phys. A: Math. Gen. **32**, 4593 (1999).
[28] C. Laing, D. W. Sumners, J. Phys. A: Math. Gen. **39**, 3535 (2006).
[29] A. Dobay, J. Dubochet, K. Millett, P.-E. Sottas, A. Stasiak, Proc. Natl. Acad. Sci. USA **100**, 5611 (2003).
[30] T. Deguchi, K. Tsurusaki, Phys. Rev. E **55**, 6245 (1997).